THEORETICAL AND EXPERIMENTAL STUDY OF HEAT DIFFUSION IN STRUCTURES WITH INTERNAL FLAWS

Sinthya Gonçalves Tavares
Departamento de Engenharia Mecânica da Universidade Federal de Minas Gerais - Av. Antônio Carlos 6627 – Pampulha – Belo Horizonte – MG – Brasil – 31270-901
gtavar@terra.com.br

Ângela Mara Cunha
Departamento de Engenharia Mecânica da Universidade Federal de Minas Gerais - Av. Antônio Carlos 6627 – Pampulha – Belo Horizonte – MG – Brasil – 31270-901
amscunha@yahoo.com.br

Roberto Márcio de Andrade
Departamento de Engenharia Mecânica da Universidade Federal de Minas Gerais - Av. Antônio Carlos 6627 – Pampulha – Belo Horizonte – MG – Brasil – 31270-901
rma@ufmg..br

Abstract. *Classified as a nondestructive thermal evaluation, NDTE, the thermography enables the conversion of thermal radiation patterns emitted by any structure, machinery, or equipment, into visible images. Such capability has led to the use of this technique in preventive and/or predictive maintenance programs in industry, and in structure integrity assessment as well. This work presents numerical and experimental results of tests performed on samples with known thermal characteristics, into which flaws of different sizes have been introduced to act as barriers to heat diffusion. The mathematical model employed use the finite-volume technique. The experimental procedures were executed in the laboratories of the Departamento de Engenharia Mecânica of Universidade Federal de Minas Gerais. The results obtained from the two methodologies are analyzed and compared.*

Keywords*: thermography, internal flaws, experimental tests, mathematical model.*

1. Introduction

Despite its being extensively presented in several works as a powerful nondestructive testing method, as a rule the experimental results obtained from application of thermography are presented in a summarized way, without being correlated to those obtained from other techniques or numerical methods. On the other hand, very few studies have presented a coherent uncertainty analysis validating the experimental results in this respect.

According to Ludwig and Teruzzi (2002), the main point for thermography validation relates to the development of an analytical or mathematical model for describing the time evolution of temperature distribution on the sample surface. Sound experimental results shall be obtained by comparing the difference in temperature (represented by the thermal contrast) between flawless and flawed areas, with the temperature difference obtained with the analytical or mathematical model. It is obvious that, for actual validation of the technique, the difference between the values obtained with both methodologies, whether for the flawless or flawed area, shall be less than the measurement uncertainty. Methodologies for determining the measurement uncertainty can be found in works such as those by Tavares and Andrade (2003) and Chrzanowski, Fischer and Matyszkiel (2000).

In this work, experimental tests were conducted on samples with known thermal characteristics, into which flaws of different sizes were introduced simulated by inserting material whose thermophysical properties differed from those of the base material, and, for practical purposes, acted as barriers to heat diffusion. The experimental results are compared to those obtained from mathematical model that used finite-volume technique.

2. Experimental Procedure

The experimental tests were performed in the laboratories of the Departamento de Engenharia Mecânica of Universidade Federal de Minas Gerais. In order to prevent sunshine reflexes on the images, the tests were carried out after sunset.

For execution of the experimental tests, a wall was built with common bricks coated with mortar. The flaws were simulated by inserting material bearing thermophysical properties different from those of the base material. For such purpose, small polystyrene plates, of different sizes, were used. The wall was divided into 5 sections, according to the distribution of the polystyrene plates, and the surface was painted. A large polystyrene plate was placed on top, to minimize heat losses in that section.

Figure 1 shows a schematic view of the wall used in the tests, with elevations given in millimeters.

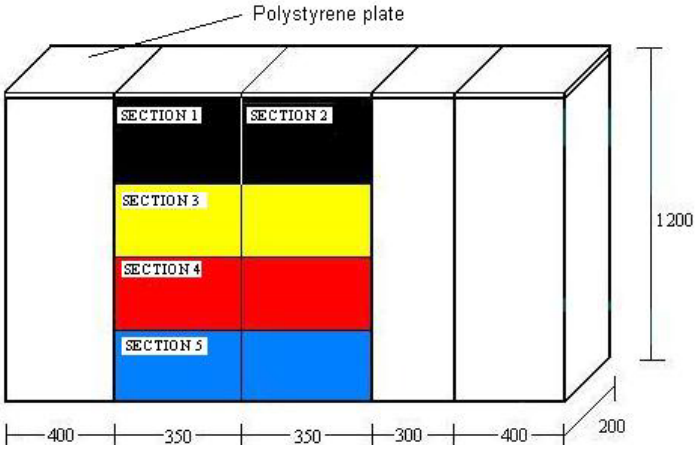

Figure 1. Wall used in the tests

On this work will be presented the results for section 2, which had been coated with a thin layer of black ink On this section the flaws were vertically aligned with those on the left side being placed between a first and a second layer of plaster, both layers being 2mm thick. On the right hand side, flaws were also inserted between two layers of plaster, with the first layer being 2mm thick, and the second, 4mm thick. The purpose was to evaluate the effect of the depth on identifying defects that is to evaluate the effectiveness of the technique in detecting flaws at greater depths.

Figure 2 presents a schematic view of this wall section, with elevations given in millimeters, which also represents the physical domain of the mathematical model. All flaws are 2mm thick and have the same edge d.

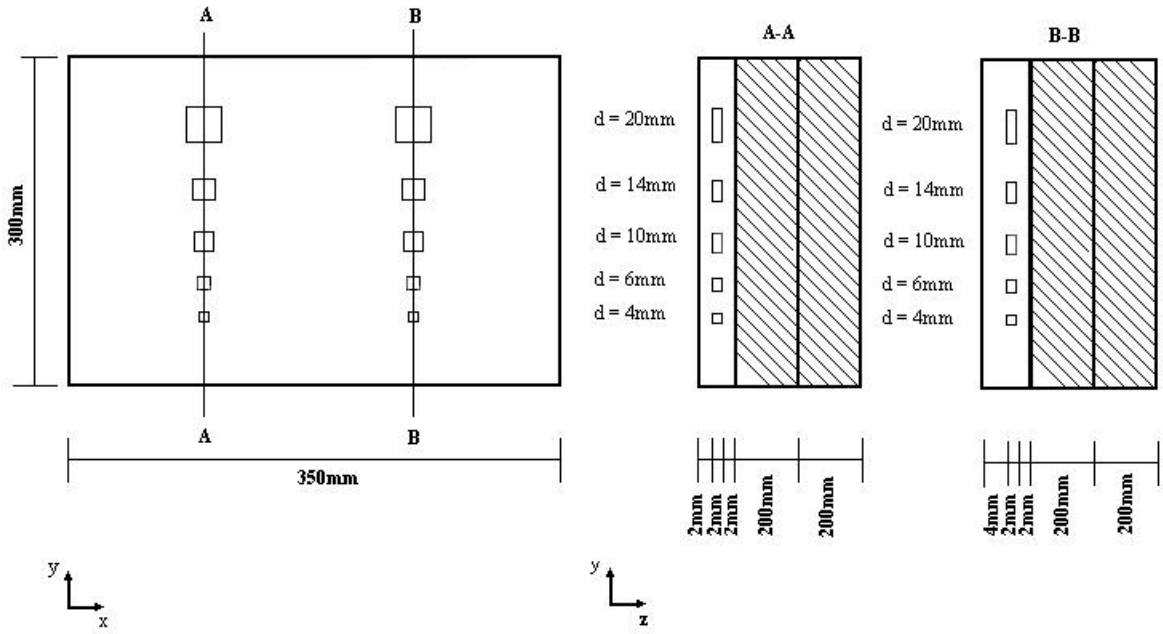

Figure 2. Flaws in detail – physical domain of the problem

The wall temperature was also monitored with K-type thermocouples installed along its surface. The data obtained from the thermocouples were used for setting up the emissivity of the surface prior to the beginning of the tests. The expanded uncertainty of the set thermocouple/temperature indicator was determined to be $\pm 0{,}2^{o}C$.

Surface emissivity of section 2, obtained during the adjustment of the thermal camera, was $0{,}96 \pm 0{,}01$, which is within the range indicated by the manufacturer of the ink used for coating the section that is $0{,}85 \pm 0{,}10$. The value indicated by Incropera and DeWitt (2003), for black ink, is 0,98.

During the tests, the ambient temperature was $19{,}1 \pm 1{,}31^{o}$ C, obtained with a thermometer whose expanded uncertainty value was $0{,}2^{o}C$ for this temperature range. Transmittance of the environment was considered to be $0{,}99 \pm 0{,}01$.

In order to obtain quantitative results, active pulsed thermography was chosen. For this, a 0,85kW electric heater, installed in areas very close to the surface being analyzed, was used. The used heating time was 1 minute, to allow uniform heating of the section under inspection. The images were taken at equal intervals during the cooling period of the section.

In order to ensure the measurement procedure repeatability, the tests were repeated 12 times, under identical testing conditions. Five images were taken for each series, representing 5 moments of the cooling of the sample.

The thermal camera AGEMA Thermovision 570, whose specifications are presented in Tab.(1), was used.

Table 1 – Characteristics of the AGEMA Thermovision 570 thermal camera

ITEM	SPECIFICATION
Operation frequency	60Hz
Focal distance	0.5m to infinite
Observable temperature range (based on black-body temperature)	- 20ºC a 1500ºC,
Measurement Uncertainty (for 30ºC in the black body)	± 0.2ºC
Viewing field	24º (horizontal) x 18º (vertical)
Detector Cooling System	Thermoelectric
Spectral response	7.5 to 13 μm;
Thermal sensitivity	< 0.15ºC

Throughout the testing, the thermal camera was placed at a distance of 1,30m from the wall, and its focal axis was kept perpendicular to the wall to minimize measurement noise. The minimum distance required between the thermal camera and the object under analysis, as described by the manufacturer, is 0,5m.

Thus the testing procedure suggested in Tavares, Andrade and Cunha (2004) was followed. With regard to uncertainty analysis, the methodology indicated in Tavares and Andrade (2003) and in Chrzanowski, Fischer and Matyszkiel (2000) was used.

3. Theoretical Model

Works such as those of Williams, Masouri and Lee (1980), Boras and Svaic (1998), and Darabi and Maldaque (2002) have presented different mathematical models for the theoretical solution of problems involving thermographic testing. However, all such works are based on the transient heat diffusion equation without heat generation, which, in three-dimensional Cartesian coordinates, is as follows:

$$\frac{\partial}{\partial x}\left(k\frac{\partial T}{\partial x}\right)+\frac{\partial}{\partial y}\left(k\frac{\partial T}{\partial y}\right)+\frac{\partial}{\partial z}\left(k\frac{\partial T}{\partial z}\right)=\rho C_p\frac{\partial T}{\partial t} \tag{1}$$

where T is the temperature (°C) at coordinates x, y, z and time, t; k is the material thermal conductivity being analyzed (W/m°C); ρ is the material specific mass (kg/m^3); and C_p is the material specific heat (J/kg°C).

For pulsed thermography, the initial conditions are as follows:

$$T(x,y,z,0)=\frac{Q}{\rho C_p\zeta} \qquad \text{for } 0<z<\zeta \tag{2}$$

$$T(x,y,z,0)=T_o \qquad \text{for } z>\zeta \tag{3}$$

where ζ is the thickness of the last layer of material which covers the surface and absorbs the thermal pulse, and T_o is the initial temperature of the samples, before thermal excitation.

The dimensions and characteristics of the wall allow to admit one-dimensional heat flow in the z direction whit boundary conditions for convection at $z=0$ *and* $z=L$, that is:

$$k\left.\frac{\partial T}{\partial z}\right|_{z=0}=h_c(T-T_\infty) \tag{4}$$

$$-k\left.\frac{\partial T}{\partial z}\right|_{z=L}=h_c(T-T_\infty) \tag{5}$$

For the convection coefficient, h_c, the value 12 W/m^2 ^{o}C was used, which is, approximately, the average of the values adopted for free gas convection in Incropera and DeWitt (2003). The ambient temperature, T_∞, used in the numerical simulation, was the average of those obtained during the experimental procedures. The properties of the materials of the wall were measured at ambient temperature during the testing. L dimensions refer to the dimensions of section 2 of the wall.

In solving Eq.(1), the numerical technique of finite-volume was used, with formulation in control volume, as proposed by Patankar (1980). The solution obtained through this technique provides perfect heat balance for the entire calculation domain.

Using the methodology suggested by Patankar (1991), a FORTRAN® program was developed for solving the problem. The number of finite control volumes was defined from grid test and convergence criterion, based on the comparison of the temperature obtained at each point, by the numerical technique, to the temperature obtained analytically (only differences of less than 10^{-5} were accepted) where the domain was considered a semi-finite solid.

4. Results

Figure 3 shows images taken during the execution of the experimental tests. The times indicated refer to the period which elapsed after the thermal source was removed.

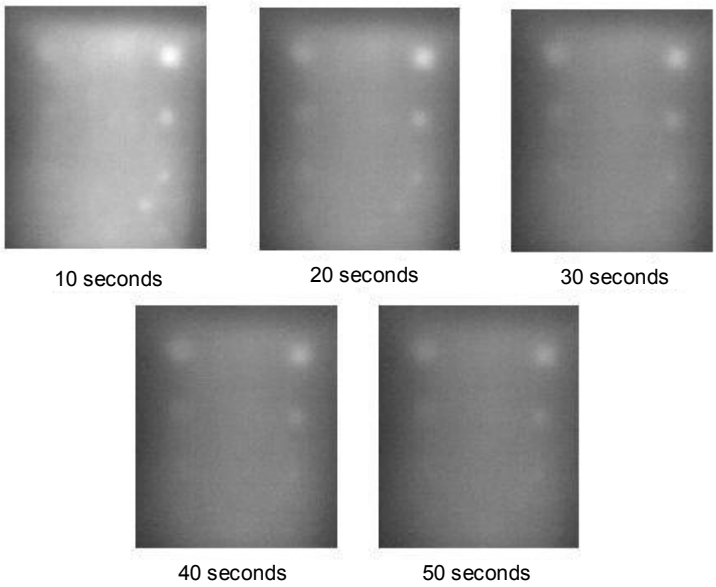

Figure 3. Thermographic images of section 2

A merely quantitative analysis of the thermographic images shows that flaws with edges of up to 10mm were perfectly visible, including those flaws located 4mm below the surface. Even with thermal contrast loss during the cooling period of the sample, the flaws remained identifiable until 40 seconds after the removal of the thermal source.

Analysis of the image yielded the temperature profile in one longitudinal portion of the section. The choice of the place within the thermographic image, for analysis of the temperature profile, was made so that such profile presented spots coinciding with the flaws. The results presented in Fig. (4) refer to images taken 20 seconds after the heat source was removed.

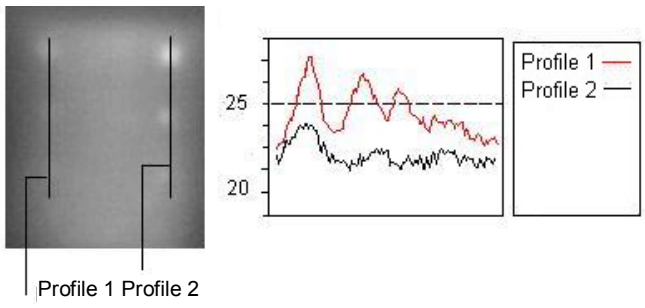

Figure 4. Temperature profile of section 2

Once again analysis of the image allowed for correct identification of flaws with edges up to 10mm, because the temperature difference between the flawless and flawed areas was greater than the measurement uncertainty, which in this case was 0.5°C.

The mathematical model allowed for a more comprehensive analysis of the changed which took place in the temperature profile of the surface over time. The results obtained by the numerical solution are presented, respectively, in Fig. (5), for the right side of the sample, where the flaws were located 4mm below the surface, and in Fig. (6), for the left side, where the flaws were 2mm below the surface.

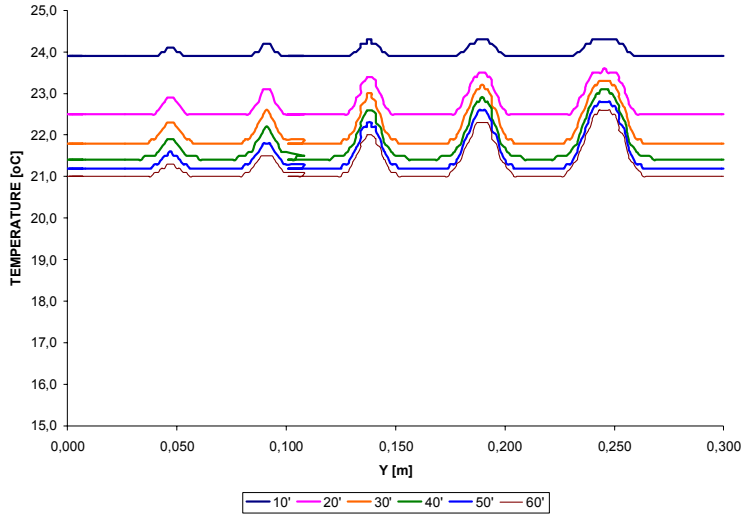

Figure 5 – Temperature profile, right side

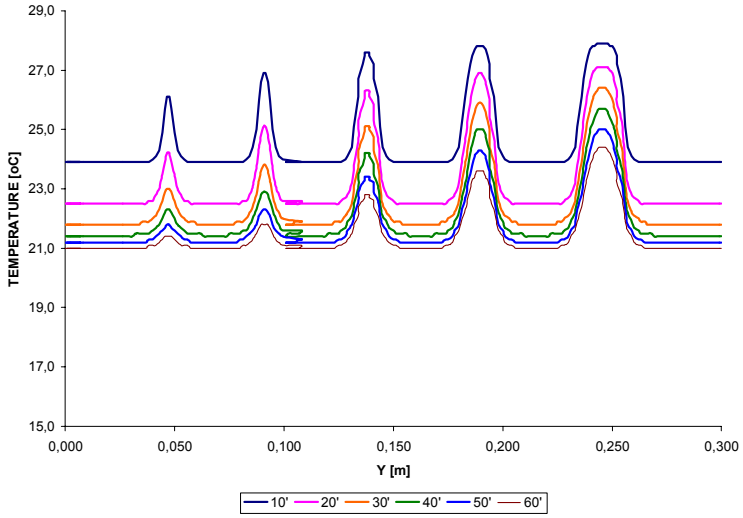

Figure 6 – Temperature profile, left side

By comparing the theoretical and experimental results, for the time period considered in the analysis of the image, it can be noticed that the difference in temperature between them, both for the flawed as for flawless area, once again was less than the measurement uncertainty, which, in principle, validates the technique. However, from the experimental viewpoint, a doubt still remains in relation to smaller edge flaws.

The mathematical model identified clearly the existence of smaller flaws, even for the right side of the sample and up to 50 seconds after the removal of the heat source. For this time period, only the temperature difference between flawless and flawed areas with 4mm edges was less than the measurement uncertainty. This is so because the mathematical model does not take into account the distance between the camera and the sample. From the experimental viewpoint, this is an important factor which becomes determinant in the quality of the image, as the energy collected by the equipment sensors is inversely proportional to the square of this distance. In other words, once each point of the thermographic image corresponds to a specific area of the surface of the measurand, an increase in distance implies that each of these points will represent a larger area of the mesurand. As a result, the radiation collected by the measuring

system is an average of the radiation emitted by this area, or, it is the average of the radiation emitted by each point of the measurand. This make that some details could be lost (Tavares, Cunha and Andrade, 2004).

Another interesting comparison can be made through the analysis of the surface temperature decay with time, for the flawless and flawed area. The numerical solution allowed for quite a comprehensive analysis of the problem and comparison with the experimental results obtained. Figures 7 and 8 present the results obtained by the mathematical model, for the right and left side of the sample respectively. Figures 9 and 10 present a comparison between the experimental results and the results from the model for the flawless and flawed section with 20mm edges.

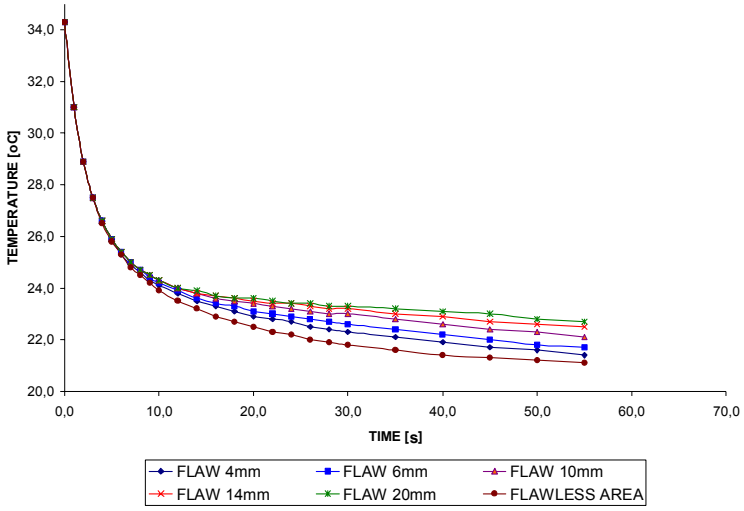

Figure 7. Temperature decay, right side

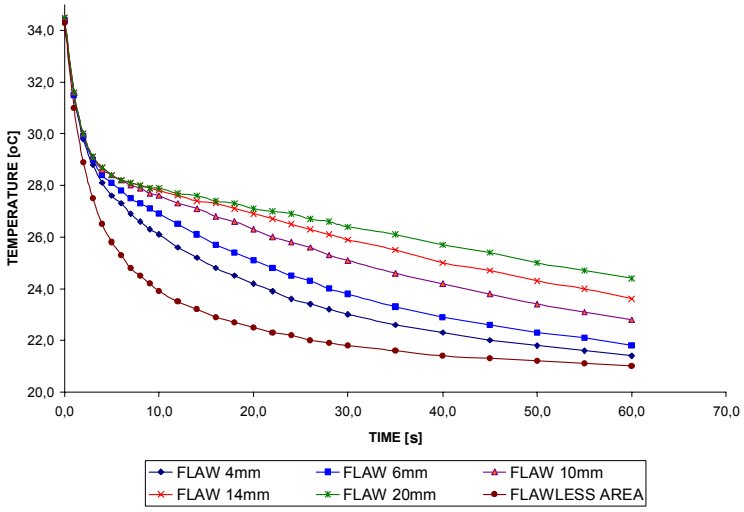

Figure 8 – Temperature decay, left side

The numerical results confirm what was expected: the bigger and more superficial flaws are more easily identified through a thermographic method, because of the larger difference in temperature between flawless and flawed areas, with regard to measurement uncertainty. On the other hand, the use of excitation methods that highlight this difference in temperature may be of interest.

Comparison between the temperature decay obtained experimentally and that obtained by the mathematical model has shown that the difference between the temperatures obtained by the two methods is within the range of measurement uncertainty. Temperature differential between flawless and flawed areas increases as non-thermal source periods also increases. Initially it was positioned at the uncertainty measurement threshold, what could give rise to doubts in relation to results if the evaluation focused only on data relative to such periods. This can be noticed in both numerical and experimental results. This phenomenon relates to thermal diffusion and to convection and radiation heat loss through surface, thus suggesting that the best time for observation is when the temperatures registered by the measurement system are duly affected by such phenomena.

The numerical technique enabled the graphical representation of the diffusion process in the sample. Figure 11 presents this process for the left hand side of the sample, in flawless sections. Figure 12, in turn, represents the diffusion process for the same side of the sample, in flawed sections.

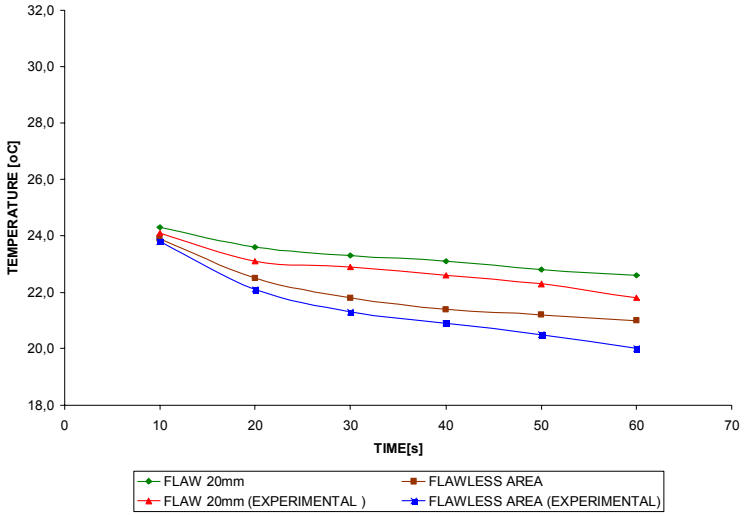

Figure 9. Temperature decay, right side – numerical x experimental

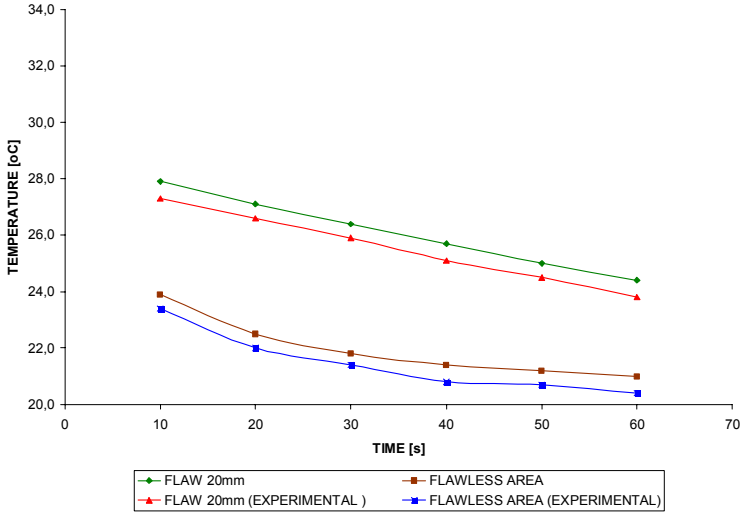

Figure 10. Temperature decay, left side – numerical x experimental

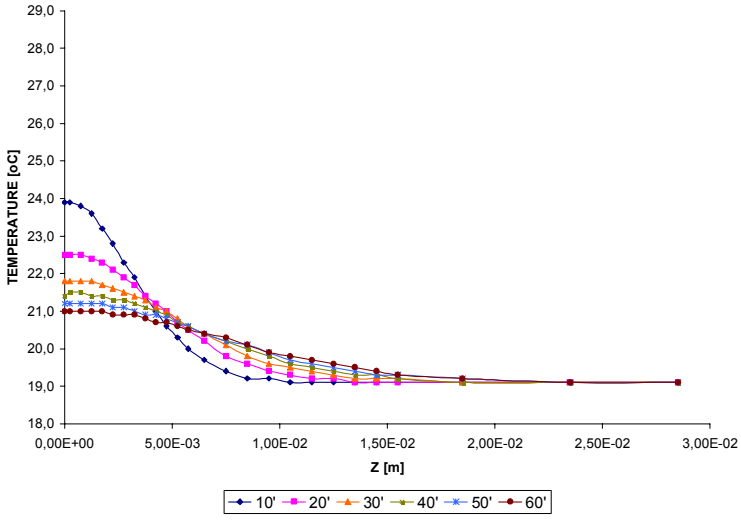

Figure 1. Diffusion process – section without flaws

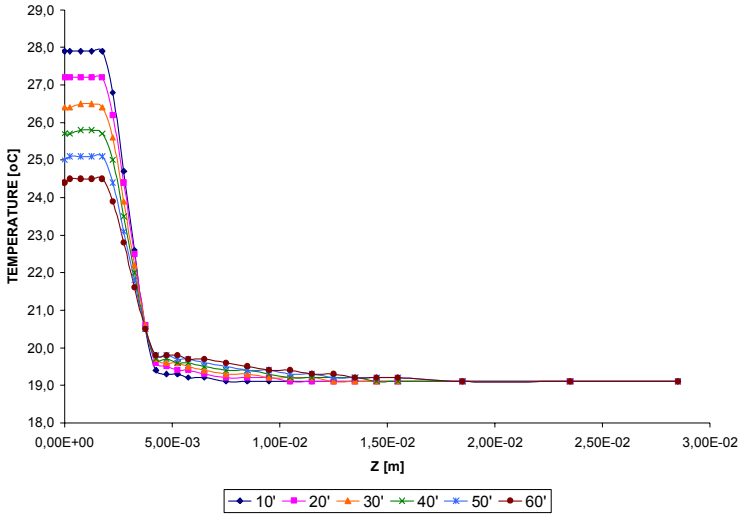

Figure 12. Diffusion process – flawed section

In Figures 11 and 12, occurrence of higher surface temperatures in the presence of flaws is clearly noticed. From a practical viewpoint, flaws constitute an obstacle to thermal diffusion, causing both this rise in surface temperature and a sudden drop in the internal temperature values which reach ambient temperature in closer-to-surface positions than when flaws are registered.

5. Conclusions

Due to innumerable advantages the thermography has been used in the most different fields of science as tool in the attainment of the transient field superficial temperature.

This study presented numerical and experimental results of tests performed on samples with known thermal characteristics, into which flaws of different sizes have been introduced to act as barriers to heat diffusion.

The experimental results, when compared to the results obtained by the mathematical model, yielded results which, on the most presented cases, validated the technique, since the difference in the temperatures obtained by the two methodologies, for both flawless and flawed areas, was within the measurement uncertainty calculated by the methodology presented in Tavares and Andrade (2003) and in Chrzanowski, Fischer and Matyszkiel (2000).

The mathematical model also contributed to a better understanding of the diffusion process and of the influence of flaws on the results obtained, for the surface temperature profile.

6. References

Boras, I., Svaic, S., "Determination of the Defect Parameters in Specimen by Means of Thermography and Numerical Methods", 1998, Proceedings of SPIE, Vol. 3396.

Chrzanowski, K., Fischer, J., Matyszkiel, R.,"Testing and evaluation of thermal cameras for absolute temperature measurement", 2000, Journal of Optical Engineering vol. 39, no 9, pp. 2535-2544.

Darabi, A., Maldague, X., 2002, Neural network based defect detection and depth estimation in TNDE", NDT&E Internacional, vol. 35, pp. 165-175.

Incropera, F. P., DeWitt, D. P., 2003, "Fundamentals of heart and mass transfer", Fifth edidtion, John Wiley & Sons, Inc., New York.

Ludwig, N., Teruzzi, P., 2002, "Heat losses and 3D diffusion phenomena for detect sizing procedures in video pulse thermography", Infrared Physics and Technology, vol. 43, pp. 297-301.

Patankar, S. V., "Numerical heat transfer and fluid flow", 1980, Hemisphere Publishing Corporation, McGrow-Hill Book co., Washington, USA.

Patankar, S. V., "Computation of Conduction and Duct Flow Heat Transfer", 1991, Innovative Research, Inc, USA, 354pp.

Tavares. S. G., Andrade, R. M., "Metodologia de ensaio e análise de incerteza na aplicação da termografia", 2003, Anais do III Congresso Brasileiro de Metrologia, Recife, PB, Brasil.

Tavares, S. G., Cunha, A. M., Andrade, R. M., "Metodologia Experimental para Aplicação da Termografia em Ensaios Térmicaos não Destrutivos", 2004, Proceedings of the 10th Congress of Thermal Sciences and Engineering – ENCIT 2004, Brazilian Society of Mechanical Sciences and Engineering, ABCM, Rio de Janeiro, Brazil.

Williams, J. H., Jr, Masouri, S. H., Lee, S. S., 1980, "One-dimensional Analysis of Thermal Nondestructive Detection of Delamination and Inclusion Flaws", British Journal of NDT, Volume 22.